Volume 21, No 3 | International Journal of Radiation Research, July 2023

Effects of high-resolution measurements between different multi-row detectors on volumetric modulated arc therapy patient-specific quality assurance

Y. Kunii[1], Y. Tanabe[2*], A. Higashi[1], A. Nakamoto[1], K. Nishioka[1]

[1]Department of Radiology, Tokuyama Central Hospital, 1-1 Kodacho, Shunan, Yamaguchi, Japan
[2]Faculty of Medicine, Graduate School of Health Sciences, Okayama University, Shikata, Kita, Okayama, Japan

► ***Original article***

Corresponding author:
Yoshinori Tanabe, Ph.D.,
E-mail:
tanabey@okayama-u.ac.jp

Received: July 2022
Final revised: December 2022
Accepted: January 2023

Int. J. Radiat. Res., July 2023; 21(3): 413-419

DOI: 10.52547/ijrr.21.3.9

Keywords: *Patient-specific QA, volumetric modulated arc therapy, single measurement, high-resolution measurement, radiation treatment planning system.*

ABSTRACT

***Background*:** This study aimed to evaluate the optimal criteria and conditions in which single-measurement (SM) and high-resolution measurement (HM) provide a similar evaluation accuracy for ArcCHECK (AC) and Octavius (OT) detectors. ***Materials and Methods*:** In the SM and HM for AC and OT, we evaluated γ-analysis pass-rate differences for various conditions (criteria, calculation grid size, and shift of the isocenter) of 20 patients who received volumetric modulated arc therapy. All results of the γ-analysis pass rate were analyzed using the Anderson–Darling normality test. ***Results*:** In the AC detector, an SM with a 1%/1 mm criterion, 1.25 mm calculation grid size, and two standard deviations (2SD) of tolerance showed an evaluation accuracy similar to that of an HM. In the OT detector, an SM with a 2%/2 mm criterion, 2.0 mm calculation grid, and 2SD of tolerance had an evaluation accuracy similar to that of an HM. The γ-pass-rate data of the OT detector for the 3%/3 mm criterion did not follow a normal distribution in both SM and HM. ***Conclusions*:** Most high γ-analysis pass rates achieved using inadequate criteria may not detect errors; therefore, accurate evaluation is necessary for optimizing the criteria settings of individual QA devices based on the characteristics and the uncertainties of array detectors. The characteristics of a detector array can be enhanced by evaluating the relationship between SM and HM, which reduces the workload of patient-specific QA.

INTRODUCTION

In volumetric modulated arc therapy (VMAT), irregularly and small shaped beam apertures are employed to minimize the risk of exposing healthy organs to radiation and focus the dose on the target [1, 2]. When using such irregularly and small shaped beam apertures, the distribution of the delivered dose by a linear accelerator may not agree with the calculated dose distribution by the radiation treatment planning system (RTPS) [3, 4].

The discordance of the dose distribution is evaluated using patient-specific quality assurance (QA) before performing VMAT [5]. Patient-specific QA is important for evaluating the dose-calculation algorithm limit, which is the detection limit of the machines that use gantry rotation speeds and multi-leaf collimator (MLC) positions [6, 7].

Instead of Gafchromic films, patient-specific QA devices are employed in two-dimensional (2D) and three-dimensional (3D) ionization chambers and diode detector arrays, such as ArcCHECK (AC) and Octavius (OT) [8]. However, detector arrays are limited by uncertainties in spatial resolution and sensitivity measurements when considering the volume and spatial arrangement of the dosimeters [9, 10]. Therefore, to effectively evaluate the VMAT dose distribution, the uncertainty of the measuring instrument must be determined and evaluated.

The optimal evaluation of VMAT, including small and irregularly shaped beam apertures, requires a high spatial resolution. By merging multiple measurements, a simple technique to achieve a high spatial resolution in detector arrays can be developed [11, 12]; this is useful for evaluating steep dose distributions, small irradiation fields, and MLC model -parameter adjustment [13]. However, multiple measurements are more time-consuming than a single measurement (SM) [14].

After conducting an acceptance test for the linear accelerator, the MLC-model parameters and tolerance limits for measurement-based QA are typically determined using multiple clinical patient cases; this may be achieved using a simple irradiation field [15]. The tolerance limit is generally determined to be two standard deviations (2SD) of the results based on the data on multiple patient measurements using the γ-index analysis pass rate [15]. The γ-index analysis can be used to evaluate the pass rate of the difference between the planned and measured dose

[DOI: 10.61186/ijrr.21.3.413]

distributions using the distance-to-agreement (DTA) and percent dose difference (DD) methods [16, 17]. For commissioning the device to be used for patient-specific QA, the SM method can be used confidently by pre-evaluating the difference between high and normal spatial resolutions for detector arrays. To the best of our knowledge, till date, no study has compared different measurement methods with two types of detector arrays for determining the optimal criteria and conditions for patient-specific QA.

Therefore, this study aimed to examine the optimal conditions in which high resolution normal resolution provides a similar evaluation accuracy in the two types of detector arrays.

METHODS AND MATERIALS

Clinical characteristics and patients

The study was approved by the Tokuyama Central Hospital Ethics Committee Review Board and adhered to the ethical guidelines of the Declaration of Helsinki (Ethical approval number: K404-20210203, Date of registration: 03/25/2022). The present study was exempted from informed consent requirements owing to its retrospective design. A total of 20 patients who were treated with VMAT from May to November 2020 were included. Among these 20 patients, treatment was performed in the head and neck regions for 10 patients, in the pelvic region for one patient, and in the prostate region for eight patients. All treatment plans were calculated using the Acuros XB calculation algorithm by the RTPS (Eclipse ver. 13.2, Varian Medical Systems, Palo Alto, CA, USA). Patient-specific QA was performed using the Novalis STx system (Varian Medical Systems, Palo Alto, CA, USA).

The patient-specific QA devices used to evaluate the plan and delivery dose distribution were the AC detector (Sun Nuclear Corp., Melbourne, FL, USA) and OT phantom (PTW, Freiburg, Germany). The AC detector is a cylindrical water-equivalent phantom with 1,386 diode detectors and is designed in a spiral pattern with a 10 mm sensor spacing. The OT phantom has an octagonal shape over its cross-section and is made of polystyrene, and a PTW 2D array (PTW, Freiburg, Germany) is inserted into it. The PTW 2D array was designed using a matrix of 729 cubic vented ionization chambers with 10 mm sensor spacing and a 5 mm cross section [18].

Two methods of measurement and γ-index analysis for the AC and OT detectors

Two measurement methods that use the AC and OT detectors for VMAT plan verification via the detector arrays are shown in figure 1. To improve the relatively large detector separation of the AC, the dose distribution of high-resolution measurement (HM) obtained using AC was merged with two dose-distribution measurements: SM (Fig. 1A) and another measurement performed by shifting the AC phantom 5 mm in the axial direction and rotating it by 2.72° (figure 1B). The HM performed using the AC detector improved the dose distribution, increasing the diagonal sampling resolution of the data from 14 to 7 mm, and the OT HM was merged with three doses (lateral axis shift of only ±5 mm of the inner device and a long axis shift of only 5 mm of the device), as shown in figures 1C and 1D. The HM of OT improved the dose distribution, increasing the diagonal sampling resolution of the data from 10 to 5 mm. The planned and measured dose distributions were evaluated through a γ-index analysis using the SNC patient software (Sun Nuclear Corporation, Melbourne, FL, USA) and VeriSoft (PTW, Freiburg, Germany) patient-analysis software. The local γ-index analysis was used to calculate the DD relative to the doses at each calculation and measurement points.

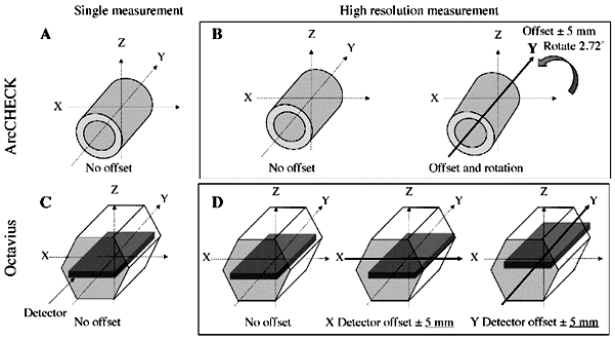

Figure 1. Illustration of the measurement method. **A:** Single measurement of ArcCHECK. **B:** High-resolution measurement of ArcCHECK. C: Single measurement of Octavius. **D:** High-resolution measurement of Octavius.

Relationship between the γ analysis pass rates for varying criteria between SM and HM

Local γ-index analysis by varying the criteria of 3%/3 mm, 2%/2 mm, or 1%/1 mm was performed for 20 patients as a pre-treatment patient-specific QA for VMAT; it measured SM and HM using the AC and OT detectors. For the γ-index analysis, we used 2D γ evaluation for AC and 3D γ evaluation for OT. A correlation analysis was performed between SM and HM for each γ value. Next, the relationship between HM and SM was evaluated using the γ pass rate under different criteria. To detect any variations from normality, all the results of the γ analysis pass rate for the varying criteria between SM and HM were analyzed by using the Anderson–Darling normality test.

Relationship between the γ analysis pass rates when varying the calculation grid size between SM and HM

The patient-specific QA plan was determined by varying the calculation grid size from 1.25 to 2.5 and 3.0 mm using RTPS. Next, the calculated QA plan was

[DOI: 10.61186/ijrr.21.3.413]

analyzed at the γ pass rates of SM and HM for each AC and OT measurement. The γ-analysis pass rate, which was measured by varying the calculated grid size, was evaluated for significant differences and compared with the control (optimal grid size at a high mean γ pass rate with each AC and OT measurement) using the nonparametric Steel test.

γ-analysis pass rate for the shifting calculated center position between SM and HM

The VMAT QA plan was determined by shifting the isocenter as a systematic error in the RTPS to evaluate the relationship between the spatial resolution and distance of the detector. The shift values were ±1.5 mm in the cranio-caudal direction, 1.5 mm in the vertical and the horizontal directions (with the 3D displacement error of 2.6 mm), followed by 2 mm in each of the three directions (with the 3D displacement error of 3.4 mm). The shifting 3D displacement error was set to approximately 3 mm; this was the boundary between the 3%/3 mm and 2%/2 mm criterion. The effects of the criteria of the AC and OT measurements were evaluated before and after shifting both SM and HM. The 2SD of the tolerance limit for the VMAT QA plan verification was calculated for all data. All the results of the γ pass rate that utilized no shift (control) and those that involved a shift were evaluated for significant differences using the nonparametric Steel test.

Statistical analysis

For statistical analysis, the r values (linear regression analysis) were determined using JMP Pro 15 (SAS, Cary, NC, USA). The Anderson–Darling normality test was used to evaluate the hypothesis of normality. Statistical significance was assessed using the Steel test in conjunction with JMP Pro 15. Results were considered to be statistically significant at p-values < 0.005.

RESULTS

Figure 2 shows the relationship between the γ-analysis pass rates of SM and HM for varying criteria. For both the AC and OT detectors, the γ-analysis pass rate decreased as the criteria became stricter (figure 2). For the AC detector, the relationships between SM and HM for the criteria of 3%/3 mm, 2%/2 mm, and 1%/1 mm were correlated at r = 0.849, 0.858, and 0.924, respectively. For the OT detector, the relationships between SM and HM for the criteria of 3%/3 mm, 2%/2 mm, and 1%/1 mm were correlated at r = 0.735, 0.925, and 0.875, respectively. The OT γ pass rate was greater than 95%, except for the case evaluated using the 3%/3 mm criterion. In the OT measurements, both SM and HM at the 3%/3 mm criterion did not follow a normal distribution (p < 0.005). The other data were normally distributed, as determined using the Anderson–Darling normality test.

Table 1 shows the changes in the γ-index analysis pass rate with the varying calculation grid sizes between SM and HM. For the AC measurements, the best mean γ analysis pass rate (3%/3 mm criterion, SM: 97.1%, and HM: 96.2%; 2%/2 mm criterion, SM: 87.7%, and HM: 86.5%) was a calculation grid size of 1.25 mm for both SM and HM (table 1). The 1.25 mm calculation grid size for both SM and HM used by the AC detector exhibited a significant difference compared with other calculation grid sizes (figure 3). In the OT measurements, the best mean γ-analysis pass rate (3%/3 mm criterion, SM: 100.0%, and HM: 99.0%; 2%/2 mm criterion, SM: 96.7%, and HM: 96.3%) was a calculation grid size of 2 mm for both SM and HM data (table 1). However, a significant difference was observed in the grid size compared with the other calculation grid sizes (3%/3-mm criterion, SM, 2 vs. 3 mm; 2%/2 mm criterion, SM, 2 vs. 1.25 and 3.0 mm; HM, 2 vs. 3 mm), as shown in figure 3.

The results of the γ-analysis pass rate for the shifting calculation isocenter position are presented in figure 4 and table 2. For a displacement error of 2.6 mm, the γ pass rate measured using the AC detector decreased by more than 10%, whereas that measured using the OT detector decreased by more than 4% (table 2). For a displacement error of 2.6 mm, the γ pass rate measured by the AC detector decreased by more than 10%, whereas that measured using the OT detector decreased by more than 4% (table 2). For a displacement error of 3.4 mm, the γ pass rate measured using the AC detector decreased by more than 21%, whereas that measured by the OT detector decreased by more than 28% (table 2). Finally, for a displacement error of 3.4 mm, both the AC and OT detectors could measure errors exceeding the 2SD tolerance limit (table 2). For the AC detector, neither SM nor HM could detect errors exceeding the 3SD tolerance limit compared with errors before the shift. However, an OT detector can detect such errors. All the results obtained for the γ pass rate, no-shift data, and shifted data were significantly different when evaluated using the nonparametric Steel test (figure 4).

DISCUSSION

SM and HM were more strongly correlated in AC for the 1%/1 mm criterion than the 2%/2 mm criterion, whereas in OT, they were weakly correlated compared with that for the 2%/2 mm criterion. The γ pass rate data obtained by the OT detector for the 3%/3 mm criterion did not follow a normal distribution, which indicates a low error detectability in determining the dosimetry QA (19, 20). This may be because the ion chamber volume of the OT detector was larger (0.125 cm3) than that of the AC detector (0.064 cm3). We consider that the high

[DOI: 10.61186/ijrr.21.3.413]

γ pass rate result for OT and a 3%/3 mm criterion does not necessarily indicate an accurate evaluation of the dose distribution between the planned and delivered doses because an accurate evaluation requires the appropriate criteria according to the characteristics of the QA device [15]. In addition, we consider that strict γ-pass criteria for patient-specific QA can be used to evaluate a fine-dose-calculation resolution and dose distributions [21].

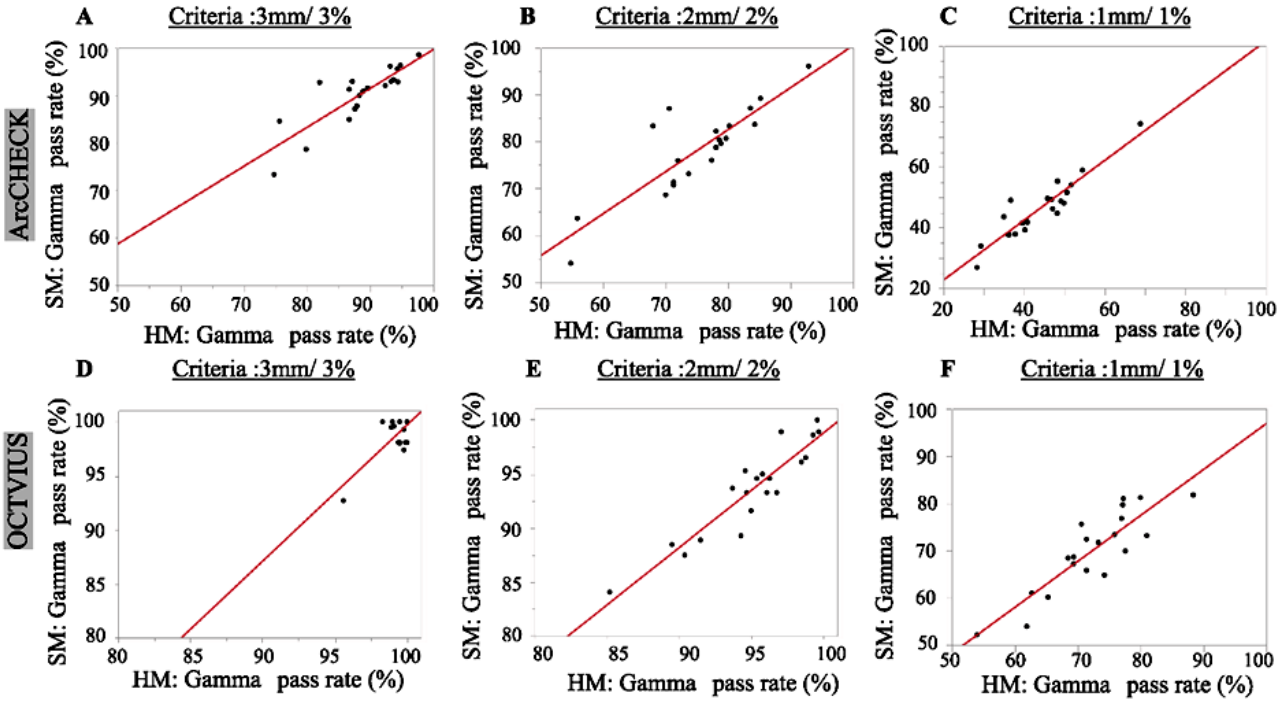

Figure 2. Relationship between the γ-analysis pass rates for a single measurement (SM) and high-resolution measurement (HM) for varying criteria. **A:** criteria 3%/3 mm, ArcCHECK. **B:** criteria 2%/2 mm, ArcCHECK. C: criteria 1%/1 mm, ArcCHECK. **D:** criteria 3%/3 mm, Octavius. **E:** criteria 2%/2 mm, Octavius. **F:** criteria 1%/1 mm, Octavius. The line represents a linear curve ($p < 0.005$).

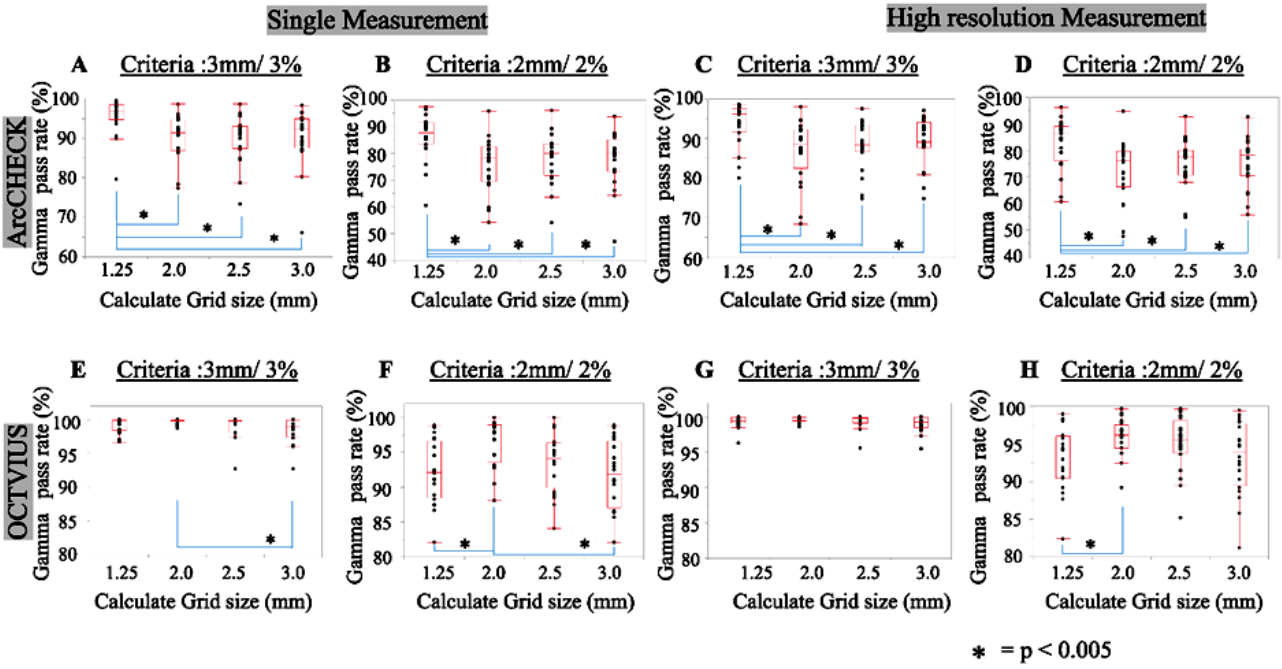

Figure 3. Relationship between the γ-analysis pass rates of a single measurement (SM) and high-resolution measurement (HM) for varying calculation grid size. **A:** SM, criteria 3%/3 mm, ArcCHECK. **B:** SM, criteria 2%/2 mm, ArcCHECK. **C:** HM, criteria 3%/3 mm, ArcCHECK. D: HM, criteria 2%/2 mm, ArcCHECK. E: SM, criteria 3%/3 mm, Octavius. F: SM, criteria 2%/2 mm, Octavius. **G:** HM, criteria 3%/3 mm, Octavius. **H:** HM, criteria 2%/2 mm, Octavius. Statistically significant differences were used the nonparametric Steel test was used ($p < 0.005$).

[DOI: 10.61186/ijrr.21.3.413]

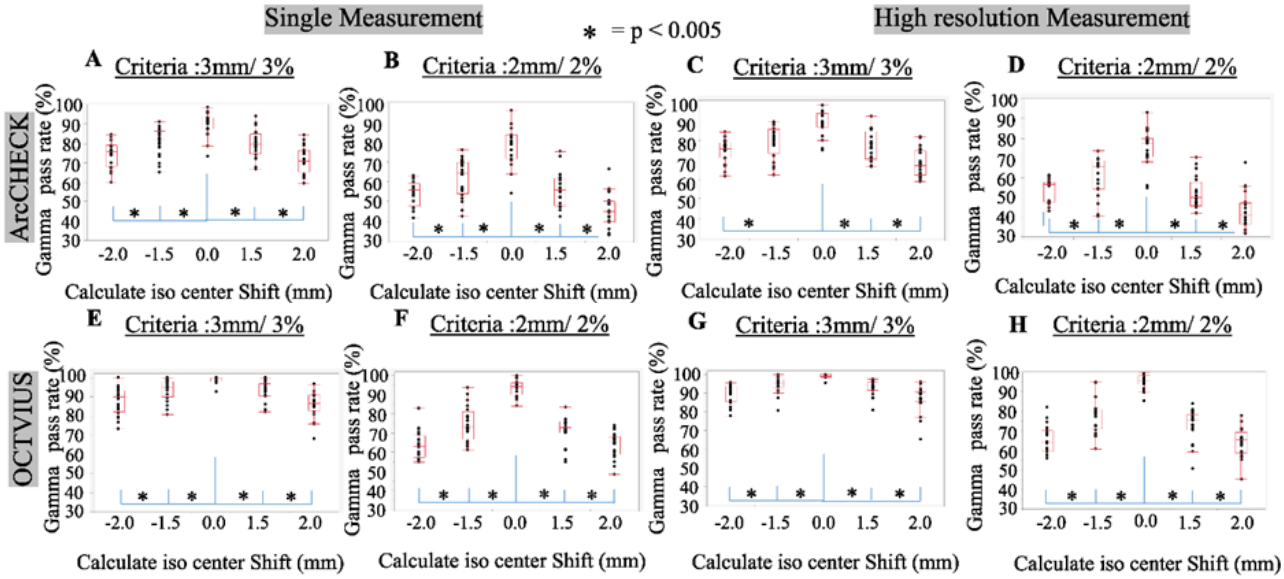

Figure 4. γ-analysis pass rate for the shifting calculation isocenter position between a single measurement (SM) and high-resolution measurement (HM). **A:** SM, criteria 3%/3 mm, ArcCHECK. **B:** SM, criteria 2%/2 mm, ArcCHECK. C: HM, criteria 3%/3 mm, ArcCHECK. **D:** HM, criteria 2%/2 mm, ArcCHECK. **E:** SM, criteria 3%/3 mm, Octavius. **F:** SM, criteria 2%/2 mm, Octavius. **G:** HM, criteria 3%/3 mm, Octavius. H: HM, criteria 2%/2 mm, Octavius. Statistically significant differences were used the nonparametric Steel test ($p < 0.005$).

Table 1. γ-analysis pass rate for varied calculation grid sizes between SM and HM.

2D array	Calculation grid size (mm)	Measurement method	Criteria: 3%/3 mm γ pass rate (%) Mean (range)	Criteria: 3%/2 mm γ pass rate (%) Mean (min–max)
ArcCHECK	1.25	SM	97.1 (79.6–99.5)	87.7 (60.5–97.4)
		HM	96.2 (80.0–98.7)	86.5 (60.7–96.3)
	2.0	SM	91.4 (77.4–98.6)	78.4 (54.2–95.8)
		HM	88.7 (68.3–98.1)	76.0 (47.6–94.8)
	2.5	SM	91.8 (73.4–98.6)	80.0 (54.1–96.1)
		HM	88.5 (74.7–97.6)	77.6 (54.7–92.8)
	3.0	SM	92.4 (66.1–98.3)	92.4 (66.1–98.3)
		HM	89.1 (74.7–89.1)	78.3 (55.8–92.6)
Octavius	1.25	SM	99.9 (96.7–100.0)	92.1 (82.1–98.8)
		HM	99.4 (96.3–100.0)	93.6 (82.4–99.0)
	2.0	SM	100.0 (98.7–100.0)	96.7 (88.1–100.0)
		HM	99.0 (98.6–100.0)	96.3 (89.2–99.7)
	2.5	SM	99.8 (92.7–100.0)	94.2 (84.1–100.0)
		HM	99.8 (95.6–100.0)	95.6 (85.2–99.7)
	3.0	SM	99.0 (92.7–100.0)	91.8 (82.1–98.9)
		HM	99.3 (95.5–100.0)	94.0 (81.2–99.5)

Table 1. γ-analysis pass rate for varied calculation grid sizes between SM and HM.

2D Array	Shift value (mm)	Measurement method	Criteria: 3%/3-mm γ pass rate (%) mean (range), SD	Criteria: 2%/2-mm γ pass rate (%) mean (range), SD	Deterioration rate from the no shift (%) Criteria A: 3%/3 mm; Criteria B: 2%/2 mm
ArcCHECK	0.0	SM	91.8 (73.4–98.6), 6.0	80.0 (54.1–96.1), 9.3	_
		HM	88.5 (74.7–97.6), 6.2	77.7 (54.7–92.8), 8.9	_
	1.5	SM	79.80 (66.8–94.1), 7.0	55.6 (42.3–75.3), 8.4	A: 12.0. B: 24.6
		HM	76.6 (66.4–92.1), 7.4	49.8 (42.1–70.2), 7.8	A: 12.0, B: 27.9
	2.0	SM	70.75 (59.6–84.4), 6.7	45.0 (32.9–66.4), 8.5	A: 21.1, B: 35.1
		HM	67.0 (58.8–81.7), 7.0	41.0 (31.7–67.5), 9.1	A: 21.6, B: 36.7
	−1.5	SM	82.1 (65.2–91.2), 9.8	64.5 (42.4–76.1), 9.8	A: 9.7, B: 15.5
		HM	81.3 (89.1–62.2), 8.4	65.5 (40.5–73.4), 8.0	A: 7.3, B: 12.2
	−2.0	SM	75.8 (60.0–84.6), 6.4	55.7 (41.6–63.1), 6.4	A: 16.0, B: 24.4
		HM	75.6 (61.6–84.1), 8.5	56.7 (43.0–61.2), 6.0	A: 13.0, B: 21.0
Octavius	0.0	SM	99.8 (92.7–100.0), 1.69	94.2 (84.1–100.0), 4.1	_
		HM	99.8 (95.6–100.0), 0.99	95.6 (85.2–99.7), 3.62	_
	1.5	SM	93.3 (82.2–100.0), 4.8	72.9 (54.8–83.5), 4.4	A: 6.5, B: 21.3
		HM	93.7 (80.8–97.6), 4.0	75.4 (50.6–83.8), 4.0	A: 6.1, B: 20.2
	2.0	SM	86.4 (68.2–48.4), 6.6	65.4 (48.4–74.0), 6.7	A: 13.4, B: 28.8
		HM	88.3 (65.2–96.1), 8.9	65.2 (45.2–77.7), 7.0	A: 11.5, B: 30.4
	−1.5	SM	95.2 (80.8–100.0), 5.5	73.6 (61.2–93.7), 8.9	A: 4.7, B: 20.6
		HM	95.4 (80.6–100.0), 4.4	77.9 (60.7–94.8), 8.5	A: 4.4, B: 17.7
	−2.0	SM	90.1 (73.3–100.0), 7.1	62.9 (54.8–82.9), 7.1	A: 9.7, B: 31.3
		HM	90.8 (77.8–97.8), 5.6	64.0 (55.9–82.0), 6.9	A: 9.0, B: 31.6

[DOI: 10.61186/ijrr.21.3.413]

Regarding the change in the dose grid, we observed that the 1.25 mm grid had the highest γ pass rate when the AC detector was used, whereas the 2 mm calculation grid had the highest γ pass rate when the OT detector was used, which may be influenced by the size of the dosimeter [22]. Moreover, the 1.25 mm grid size used with the AC detector exhibited significantly different γ pass rates from the other grid sizes. The 2.0 mm grid size used with the OT detector exhibited a significant difference in the γ pass rate for specific conditions. In addition to the significance of the small dosimeter, this phenomenon may be affected by the low γ pass rate of the AC detector (table 1). These results demonstrate that if the pass rate is adequately low, slight DTA and percent DD errors can be easily detected with high sensitivity [21, 22]. Furthermore, the 3D γ evaluation increased the evaluation accuracy of this system, and the γ pass rate of the OT detector is expected to improve compared with the 2D γ evaluation of the AC detector [23, 24]. To determine the optimal QA criteria, we must carefully consider the uncertainty of the evaluation mode and calculation grid. The γ-analysis pass rate considerably decreased for a displacement error of 2.6 mm when using AC compared with that for OT . In addition, the 3D displacement error of 3.4 mm could detect the 2SD of tolerance in both the AC and OT detectors. For detection at 2SD, the setting of the facility must be adjusted based on the evaluation method and criteria, and the apparatus should be assessed for evaluation limit prior to clinical use [25, 26]. When the γ-analysis pass rate of the 3D displacement error in the AC was 3.4 mm, neither SM nor HM could detect errors exceeding 3SD after the shift; conversely, OT could detect these errors under the same conditions. The physical distance from the top surface of the AC to the detector is 2.9 cm [11], which is shallower than that of the OT detector. The error of the AC detector may result in smoothness farther (20.8 cm) from the entrance/exit dosimeter as well as field-size dependencies [9, 27].

However, as a limitation of this study, we were unable to evaluate the differences in dose distributions between SM and HM. In addition, HM included the burden of patient-specific QA during multiple measurements. In this study, the γ pass rate exhibited a correlation with SM, and it was observed that only SM can be used to detect the 2SD of the tolerance by evaluating the optimal criteria and calculation grid. The high-resolution mode is considered useful for evaluating errors in greater detail beyond 2SD for patient-specific QA [25].

In the future, a high spatial resolution may be achieved from normal spatial-resolution data using artificial intelligence and MLC log files, which may lead to reduced workloads and more accurate evaluations [28-31].

CONCLUSIONS

The results of the study suggested that SM and HM can achieve the same evaluation accuracy with 1%/1 mm criterion, 1.25 mm calculation grid size for AC, 2%/2 mm criterion, and 2.0 mm calculation grid for OT. A comprehensive analysis of multiple measurements for the detector array is useful for determining the appropriate QA-criterion settings and conditions based on the uncertainty of QA devices for use in patient-specific QA.

Funding: The authors did not receive support from any organization for the submitted work.

Competing interests: The authors have no relevant financial or non-financial interests to disclose.

Availability of data and material: Not applicable.

Code availability: Not applicable.

Authors' contributions: All authors contributed to the manuscript equally.

Ethics approval: The study was approved by the Ethics Committee of the Institutional Review Board of Tokuyama Central Hospital, and it conformed to the ethical guidelines of the Declaration of Helsinki (K404 - 20210203, Date of registration: March / 25 / 2022).

Consent to participate: The IRB waived the need to obtain patient consent, owing to the retrospective nature of the study.

Consent for publication: Not applicable.

REFERENCES

1. Ezzell GA, Galvin JM, Low D, *et al.* (2003) Guidance document on delivery, treatment planning, and clinical implementation of IMRT: report of the IMRT Subcommittee of the AAPM Radiation Therapy Committee. *Med Phys, **30**(8): 2089-2115*.
2. Zhang P, Happersett L, Hunt M, *et al.* (2010) Volumetric modulated arc therapy: planning and evaluation for prostate cancer cases. *Int J Radiat Oncol Biol Phys, **76**(5): 1456-1462*.
3. Du W, Cho SH, Zhang X, *et al.* (2014) Quantification of beam complexity in intensity-modulated radiation therapy treatment plans. *Med Phys, **41**(2): 021716*.
4. Park JM, Park SY, Kim H (2015) Modulation index for VMAT considering both mechanical and dose calculation uncertainties. *Phys Med Biol, **60**(18): 7101-7125*.
5. Fredh A, Scherman JB, Fog LS, Munck af Rosenschöld P (2013) Patient QA systems for rotational radiation therapy: a comparative experimental study with intentional errors. *Med Phys, **40**(3): 031716*.
6. Otto K (2008) Volumetric modulated arc therapy: IMRT in a single gantry arc. *Med Phys, **35**(1): 310-317*.
7. Yassin A, Elshahat KM, Attlah EM, *et al.* (2021) Dose verification and plan conformity with three different dosimeters for intensity-modulated radiation therapy plans. *Int J Radiat Res, **19**(3): 703-710*.
8. Hussein M, Adams EJ, Jordan TJ, *et al.* (2013) A critical evaluation of the PTW 2D-ARRAY seven29 and OCTAVIUS II phantom for IMRT and VMAT verification. *J Appl Clin Med Phys, **14**(6): 274-292*.
9. Feygelman V, Zhang G, Stevens C, Nelms BE (2011) Evaluation of a new VMAT QA device, or the "X" and "O" array geometries. *J Appl Clin Med Phys, **12**(2): 3346*.
10. Masi L, Casamassima F, Doro R, Francescon P (2011) Quality assurance of volumetric modulated arc therapy: evaluation and comparison of different dosimetric systems. *Med Phys, **38**(2): 612-621*.

[DOI: 10.61186/ijrr.21.3.413]

11. Stelljes TS, Harmeyer A, Reuter J, Looe HK, Chofor N (2015) Dosimetric characteristics of the novel 2D ionization chamber array OCTAVIUS Detector 1500. *Med Phys,* ***42****(4): 1528-1537*.
12. Sun Nuclear Corporation (n.d.) ArcCHECK reference guide. Sun Nuclear Corp., Melbourne, FL, USA.
13. Kinsella P, Shields L, McCavana P, McClean B, Langan B (2016) Determination of MLC model parameters for Monaco using commercial diode arrays. *J Appl Clin Med Phys,* ***17****(4): 37-47*.
14. Pan Y, Yang R, Zhang S, *et al.* (2019) National survey of patient specific IMRT quality assurance in China. *Radiat Oncol,* ***14****(1): 69*.
15. Miften M, Olch A, Mihailidis D, *et al.* (2018) Tolerance limits and methodologies for IMRT measurement-based verification QA: recommendations of AAPM Task Group No. 218. *Med Phys,* ***45****(4): e53-e83*.
16. Low DA, Harms WB, Mutic S, Purdy JA (1998) A technique for the quantitative evaluation of dose distributions. *Med Phys,* ***25****(5): 656 -661*.
17. Park JM, Kim JI, Park SY, *et al.* (2018) Reliability of the gamma index analysis as a verification method of volumetric modulated arc therapy plans. *Radiat Oncol,* ***13****(1): 175*.
18. Poppe B, Blechschmidt A, Djouguela A, et al. (2006) Two-dimensional ionization chamber arrays for IMRT plan verification. *Med Phys,* ***33****(4): 1005-1015*.
19. Heilemann G, Poppe B, Laub W (2013) On the sensitivity of common gamma index evaluation methods to MLC misalignments in Rapidarc quality assurance. *Med Phys,* ***40****(3): 031702*.
20. Mu G, Ludlum E, Xia P (2008) Impact of MLC leaf position errors on simple and complex IMRT plans for head and neck cancer. *Phys Med Biol,* ***53****(1): 77-88*.
21. Chun M, Kim JI, Oh DH, *et al.* (2020) Effect of dose grid resolution on the results of patientspecific quality assurance for intensity-modulated radiation therapy and volumetric modulated arc therapy. *Int J Radiat Res,* ***18****(3): 521-530*.
22. Yasui K, Saito Y, Ogawa S, Hayashi N (2021) Dosimetric characterization of a new two-dimensional diode detector array used for stereotactic radiosurgery quality assurance. *Int J Radiat Res,* ***19****(2): 281-289*.
23. Kim JI, Choi CH, Wu HG, *et al.* (2016) Correlation analysis between 2D and quasi-3D gamma evaluations for both intensity-modulated radiation therapy and volumetric modulated arc therapy. *Oncotarget,* ***8(3):*** *5449-5459*.
24. Persoon LCGG, Podesta M, van Elmpt WJC, *et al.* (2011) A fast three-dimensional gamma evaluation using a GPU utilizing texture memory for on-the-fly interpolations. *Med Phys,* ***38****(7): 4032-4035*.
25. Kunii Y, Tanabe Y, Nakamoto A, Nishioka K (2022) Statistical analysis of correlation of gamma passing results for two quality assurance phantoms used for patient-specific quality assurance in volumetric modulated arc radiotherapy. *Med Dosim,* ***47****(4): 329-333*.
26. Esmaili G, Mahdavi SR, Nikoofar AR, *et al.* (2018) Dosimetric verification of pre-treatment intensity modulated radiation therapy in the commissioning process. *Int J Radiat Res,* ***16****(4): 493-497*.
27. Neilson C, Klein M, Barnett R, Yartsev S (2013) Delivery quality assurance with ArcCHECK. *Med Dosim,* ***38****(1): 77-80*.
28. Nelms BE, Zhen H, Tomé WA (2011) Per-beam, planar IMRT QA passing rates do not predict clinically relevant patient dose errors. *Med Phys,* ***38****(2): 1037-1044*.
29. Valdes G, Scheuermann R, Hung C, Olszanski A, *et al.* (2016) A mathematical framework for virtual IMRT QA using machine learning. *Med Phys,* ***43****(7): 4323-4334*.
30. Tanabe Y, Ishida T, Eto H, *et al.* (2021) Patient-specific radiotherapy quality assurance for estimating actual treatment dose. *Med Dosim,* ***46****(1): e5-e10*.
31. Osman AFI, Maalej NM, Jayesh K (2020) Prediction of the individual multileaf collimator positional deviations during dynamic IMRT delivery priori with artificial neural network. *Med Phys,* ***47****(4): 1421 -1430*.

[DOI: 10.61186/ijrr.21.3.413]